

# On the ringdown transient of transformers

N. Chiesa, A. Avendaño, H. K. Høidalen, B. A. Mork, D. Ishchenko, and A. P. Kunze.

**Abstract**—This paper details the analysis of transformer ringdown transients that determine the residual fluxes. A novel energy approach is used to analyze the causes of transformer saturation during de-energization. Coupling configuration, circuit breaker and shunt capacitor influence on residual flux have been studied. Flux-linked initialization suggestions are given at the end of the paper.

**Keywords:** Power transformer, inrush current, ringdown transient, residual flux, shunt capacitance.

## I. INTRODUCTION

THE energization of a power transformer may result in a severe inrush current. A power transformer inrush current is characterized by a high magnitude of the current first peak. This current is damped by the dissipative elements of the transformer and reaches a steady state value after several cycles. The first peak can be in the same order of magnitude as the transformer short circuit current and may cause undesirable events (false operations of protective relays, mechanical damages to the transformer windings, excessive stress on the insulation and voltage dips that can influence the system's power quality).

The scientific community is well aware of this problem and many papers have been published concerning inrush current estimation, modeling and mitigation [1]–[6]. Inrush current worst case is generally estimated based on air core inductance method. The modeling of energization transients is challenging and is an active topic in the research community; the preferred way of limiting inrush currents has been moved from resistor burden and shunt capacitor, to more effective synchronized switching techniques. However, optimal reduction of the stresses can be achieved only with an accurate knowledge of the residual fluxes.

Residual fluxes are due to the remnant magnetization of the core, after a transformer has been deenergized. The residual flux pattern is mostly unknown or not known precisely due to the complexity of the ringdown transient itself [5]. Ringdown transients are a little known issue and a proper understanding of these phenomena is of great importance for establishing system protection schemes and relay reclosing time philosophies, particularly in cases where shunt capacitor banks are installed on transmission lines.

N. Chiesa and H. K. Høidalen are with the Department of Electric Power Engineering, Norwegian University of Technology (NTNU), Trondheim, Norway (e-mail of corresponding author: nicola.chiesa@elkraft.ntnu.no).

A. Avendaño, B. A. Mork, D. Ishchenko and A. P. Kunze are with the Department of Electrical and Computer Engineering, Michigan Technological University (MTU), Houghton, MI 49931 USA.

Presented at the International Conference on Power Systems Transients (IPST'07) in Lyon, France on June 4-7, 2007

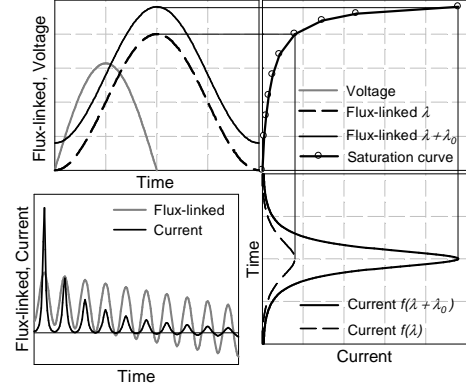


Fig. 1. Qualitative representation of the inrush current phenomenon; the effect of the residual flux.

The purpose of this paper is to investigate the ringdown phenomenon that occurs when a transformer is deenergized and leads to the creation of residual fluxes.

## II. THE RINGDOWN TRANSIENT PHENOMENA

The residual flux value is a fundamental parameter during the re-energization of a transformer since it affects the first peak of the inrush current. Assuming a sinusoidal waveform and neglecting the dissipative elements, it is possible to outline the fundamental relations that lead to the creation of an inrush current:

$$v(t) = \hat{v} \sin(\omega t + \phi) \quad (1)$$

$$\begin{aligned} \lambda(t) &= \lambda_0 + \int_0^t v(t) dt = \\ &= \lambda_0 + \frac{\hat{v}}{\omega} (\cos(\phi) - \cos(\omega t + \phi)) \end{aligned} \quad (2)$$

$$i(t) = L(\lambda) \lambda(t) \quad (3)$$

where  $\lambda_0$  is the residual flux present at the energization instant. Fig. 1 qualitatively represents the inrush current worst case; with  $t = \frac{T}{2}$  and  $\phi = 0$ , (2) becomes:

$$\lambda(T/2) = \lambda_0 + 2 \frac{\hat{v}}{\omega} = \lambda_0 + 2 \hat{\lambda} \quad (4)$$

with  $\hat{\lambda} = \frac{\hat{v}}{\omega}$  being the peak of the rated flux-linked. Thus, switching at zero voltage crossing causes the doubling of the flux-linked first-peak.

Due to the flat nature of the saturation curve, a small increase of flux peak (residual flux) can drive the iron core of the transformer into heavy saturation. The plot in the lower left corner of Fig. 1 shows a complete inrush transient and can be noticed how the DC flux offset is slowly damped to zero together with the current by the dissipative elements as winding resistance and core losses. Winding resistance has more importance in the initial part of the ringdown: high current produces high  $Ri^2$  losses. Hysteresis losses do not

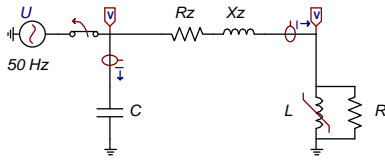


Fig. 2. ATP circuit for inrush/ringdown transient simulations.

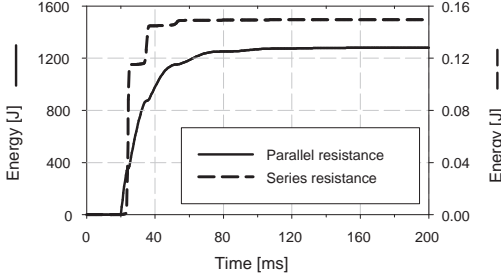


Fig. 3. Simulation of energy dissipated from the resistive elements, ( $C = 5 \mu\text{F}$ ); 290-MVA transformer.

add noticeable damping to the inrush current and only affect the magnitude of the residual magnetization [7].

The residual flux is created when a transformer is disconnected from the power grid. At the end of a de-energization transient both the voltages and currents decrease to zero, however the flux in the core retains a certain value defined as residual flux. A ringdown transient is a natural LC response that appears as the stored energy dissipates whenever a transformer is deenergized and can be simulated with the ATP/EMTP circuit shown in Fig. 2. The transformer core has been modeled with a type-98 nonlinear inductor ( $L$ ) and a linear resistor ( $R$ ). The use of a non-hysteretic inductor does not allow the estimation of residual flux. ATP offers a type-96 hysteretic inductor, however it has been dismissed due to the proved poor quality of this model [8]–[10]. The transformer short circuit impedance is modeled by the winding resistance ( $R_Z$ ) and the leakage reactance ( $X_Z$ ). Sources of capacitance ( $C$ ) include transformer winding capacitances, capacitor banks, and transmission lines and cables connected to the transformer terminals during the de-energization. The parameters of the circuit are extracted from a 290-MVA three-phase power transformer whose test report is shown in Tab. I in the Appendix.

Fig. 3 shows the energy dissipated by the resistive elements of the circuit during a ringdown transient. The energy dissipated by the series resistance ( $R_Z$ ) is much smaller than the one dissipated by the parallel resistance ( $R$ ). Thus, the circuit can be simplified in a parallel RLC circuit, disregarding the series resistance and reactance ( $R_Z = 0$  and  $X_Z = 0$ ).

Fig. 4 shows the energy dissipated by the resistance and stored in the reactive elements of the circuit in steady state conditions. The energy dissipated constantly increases as it represents the active energy drawn from the source and consumed by the circuit (losses). The analysis of the energy stored in the capacitor ( $E_C$ ) and in the inductor ( $E_L$ ) is of particular interest and three main situations can be pointed out:

- maximum energy stored in the capacitor:  $E_C = \max$ ,  $E_L = 0$ , voltage peak ( $t_{SW} = 20 \text{ ms}$ );
- maximum energy stored in the inductor:  $E_L = \max$ ,  $E_C = 0$ , voltage zero crossing ( $t_{SW} = 25 \text{ ms}$ );

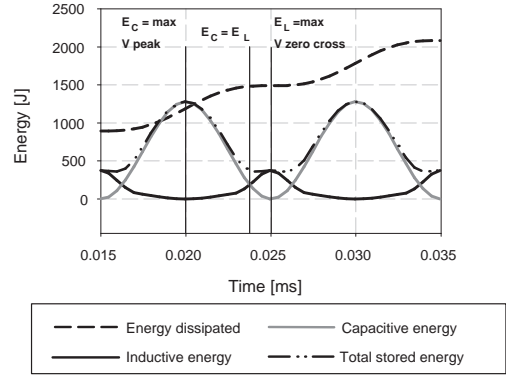


Fig. 4. Simulated energy at steady state ( $C = 5 \mu\text{F}$ ); 290-MVA transformer.

- equal energy stored in capacitor and inductor:  $E_C = E_L$  ( $t_{SW} = 23.75 \text{ ms}$  for this particular L-C configuration).

Fig. 5 shows the energy transient when the circuit is switched out at these three different instants. At any instant during the transient the energy conservation law is valid:

$$E_R + E_C + E_L = 0 \quad (5)$$

with  $E_R$  being the energy dissipated by the resistor. A comparison of Figs. 4 and 5 reveals that the total energy dissipated by the resistor is equal to the total energy stored at steady state by the reactive elements of the circuit:

$$|E_C(t_{SW}) + E_L(t_{SW})| = |E_R(t_\infty) - E_R(t_{SW})| \quad (6)$$

with  $t_{SW}$  being the switching instant and  $t_\infty$  being the end of the transient. When switching at voltage peak the net energy released by the inductor is zero. However, during the transient some energy is exchanged between the capacitor and the inductor. Analogous considerations can be made for the second case, with switching at zero voltage. For this particular configuration the maximum energy stored in the inductor is smaller than the maximum energy stored in the capacitor causing lower energy dissipation in the resistive element. Due to the nonlinear characteristic of the inductor the point where  $E_C = E_L$  does not always represent the minimum total energy stored as in a linear system.

Fig. 6 shows flux-linked and current ringdown transients for different values of capacitance  $C$ , zero crossing and peak voltage switching instants. It is important to notice how the ringdown natural frequency decreases as the value of the capacitance increases. For a parallel RLC circuit the ringdown characteristic is described by:

$$\omega_0 = \frac{1}{\sqrt{L(i)C}} \quad (7)$$

$$\alpha = \frac{1}{2RC} \quad (8)$$

$$\omega_N = \sqrt{\omega_0^2 - \alpha^2} \quad (9)$$

$$\xi = \frac{\alpha}{\omega_0} = \frac{1}{2R} \sqrt{\frac{L(i)}{C}} \quad (10)$$

where  $\omega_0$  is the undamped resonant frequency,  $\alpha$  is the damping coefficient,  $\omega_N$  is the natural frequency, and  $\xi$  is the damping ratio ( $\xi < 1$  underdamped,  $\xi = 1$  critically damped,

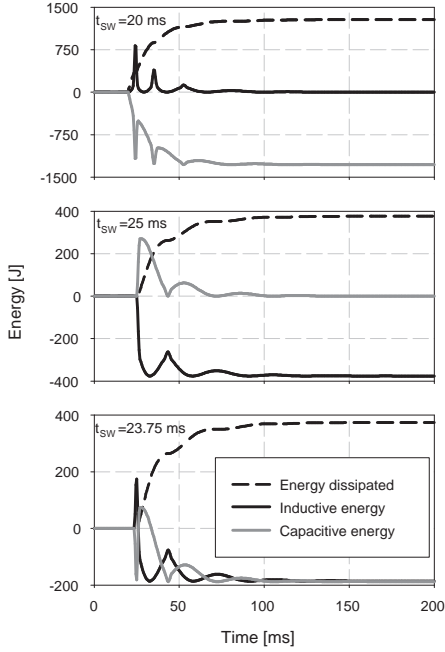


Fig. 5. Simulation of energy during ringdown transients at different disconnection instants ( $C=5 \mu\text{F}$ ), 290-MVA transformer.

$\xi > 1$  overdamped). Due to the large winding capacitance, large transformers usually have  $\xi \ll 1$  thus  $\omega_N \approx \omega_0$ . A higher value of capacitance reduces the value of the damping coefficient  $\alpha$ , increasing the duration of the ringdown transient. For a fixed value of inductance, the ringdown natural frequency will be inversely proportional to the square root of the installed capacitance. In case of a nonlinear inductance the value of the synchronous frequency  $\omega_N$  is not constant. The minimum of the natural frequency ( $\omega_{N \min}$ ) is obtained when the magnetization level is small enough and the inductance is magnetized in the linear area of the saturation curve.

A lower natural frequency causes a higher flux density in the core. However, it is inaccurate to deduce that this is the cause of the increase of flux-linked and current peaks as shown in Fig. 6 ( $C = 5 \mu\text{F}$  and  $10 \mu\text{F}$  with  $t_{\text{SW}} = 20 \text{ ms}$ ). Due to the nonlinearity of the core inductance, the natural frequency ( $\omega_N$ ) reduces from the synchronous frequency ( $\omega_S = 50 \text{ Hz}$ ) to the minimum natural frequency ( $\omega_{N \min}$ ). Fig. 7 shows that

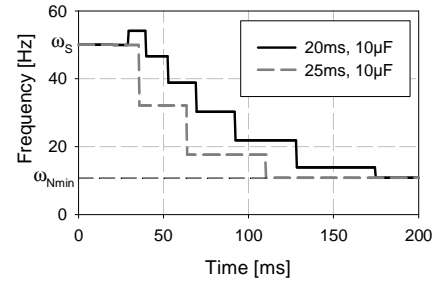


Fig. 7. Simulation of frequency variation during ringdown; 290-MVA transformer.

the time (resolution = one half period) required to reach the minimum natural frequency is not constant and is related to the disconnection instant. Since the minimum natural frequency is reached at the end of the de-energization transient, the gradual reduction of the frequency cannot justify the core saturation.

Referring to Figs. 4 and 5, and disconnection instant  $t_{\text{SW}} = 20 \text{ ms}$ , the total energy at the disconnection instant is equal to the maximum capacitive energy. After a quarter of period some of the capacitive energy has been dissipated by the resistive element, but the remaining energy must be transferred to the inductance. This quota part is higher than the maximum steady state inductive energy. In order to store a larger amount of energy in the same inductor the current has to increase considerably:

$$E_L = \frac{1}{2} L I^2 \quad (11)$$

The effect is emphasized by the nonlinear characteristic of the inductor. Thus, core saturation during ringdown is experienced only when the total energy stored in the reactive elements (inductances and capacitances) at the disconnection instant is higher than the maximum inductive energy at steady state.

### III. LABORATORY MEASUREMENTS

Laboratory measurements of residual flux have been performed on three distribution transformers with the following characteristics:

- 3-legged, 15-kVA, 60 Hz, 240(120)/208 V, Dyn/Yyn ;
- 5-legged, 150-kVA, 60 Hz, 12470/208 V, YNYn (with an airgap between the main legs and the outer legs);
- 3-legged, 500-kVA 60 Hz, 21600(12470)/480 V, YNyn/Dyn (amorphous core).

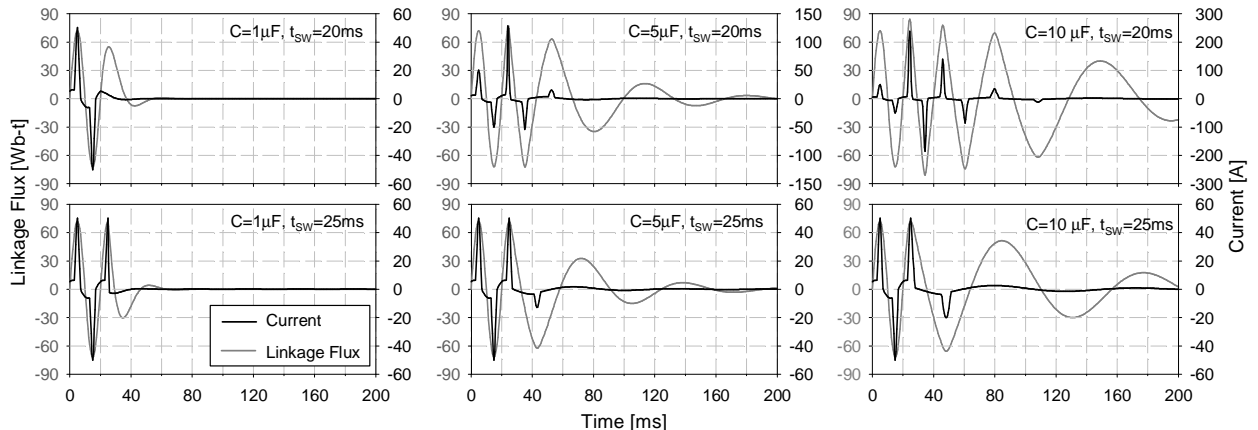


Fig. 6. Simulation of flux-linked and current waveforms during ringdown; 290-MVA transformer.

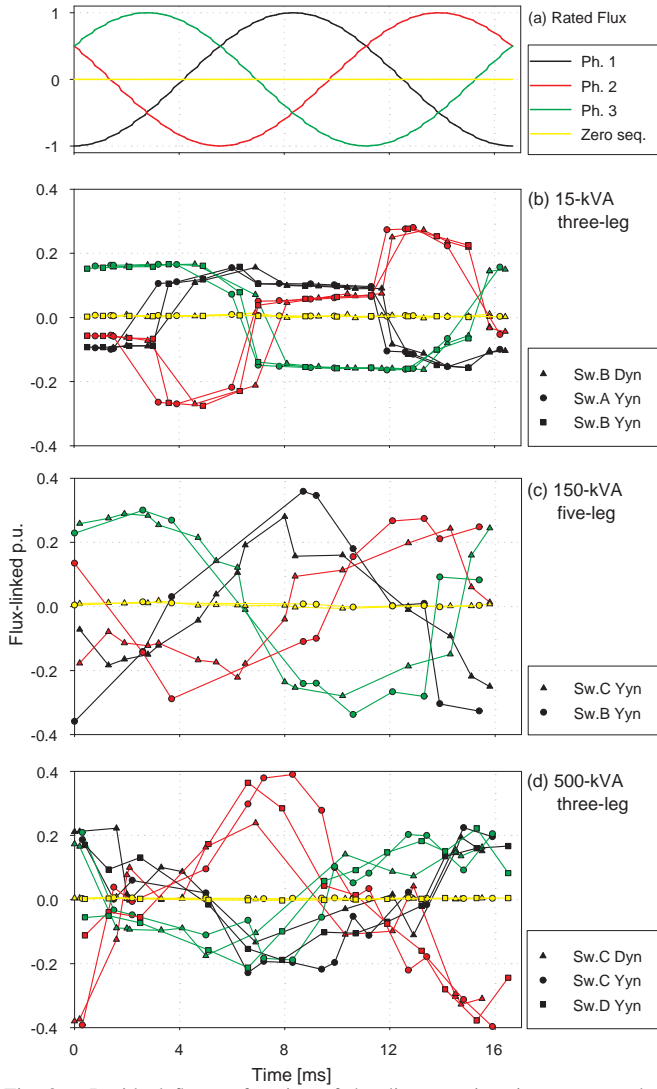


Fig. 8. Residual flux as function of the disconnection time; measured on 15-150-500 kVA transformers.

Two series of tests have been performed to analyze specific behaviors of the ringdown transient. In the first test a total of four different types of molded-case circuit breakers have been used to examine the relation between the results and the switching gear used. The impact of the winding connection configuration is also verified. The second set of tests studies the influence of shunt capacitances on the ringdown transient.

#### A. Connection configuration and circuit breaker influence

Fig. 8 shows the relation between residual fluxes (calculated from the integral of the phase voltage) of the different phases as function of the disconnection instant for the 15-kVA, 150-kVA and 500-kVA transformer respectively. No synchronized switching device has been used; the various points have been measured with random operations of the circuit breakers. An alternative to Fig. 8 is to establish a complementary cumulative probability distribution to answer how often the residual flux is above a particular level, but in this case the phase correlation is lost.

The results of these tests show that the maximum residual flux lies between 0.2 and 0.4 p.u. of the rated flux-linked. Moreover, the maximum residual flux of the central phase

results slightly higher than in the other two phases for the 15 and 500-kVA transformers.

For the smallest test object the curves representing the residual magnetization as function of the disconnection instant are in phase with the rated flux waveforms. The phase correlation is reduced as the rating of the transformer increases. With the increase of the transformer's physical size, the winding size increases, leading to an increased winding capacitance. The winding capacitance of the 15-kVA transformer is very low so the circuit behaves as a pure inductive circuit instead as a parallel LC circuit. A breaker is unable to chop an inductive current, thus the disconnection is postponed until the first current zero crossing. In a parallel LC circuit the current can be chopped since the parallel capacitance provides an alternative circulation path for the current. This has been verified analyzing the line current waveforms of the three transformers: the currents are not chopped for the 15-kVA transformer, but are chopped for the two larger transformers. Moreover, when a shunt capacitor is attached to the terminal of the 15-kVA transformer, tests have shown that the currents are chopped and the residual flux is not anymore in phase with the rated flux and resembles more the behavior seen in the larger transformers.

The sum of the residual flux is always zero. This means that no zero sequence flux is present during the ringdown transient. A three-legged core inhibits zero sequence flux because it constrains the sum of the flux to be equal to zero and potential flux in the air cannot retain magnetization. A delta winding has an analogous effect imposing the sum of the voltages to be zero. In the case of five-legged core without any delta winding, a zero sequence residual flux cannot be neglected as it can be stored in the outer legs. However, the particular core configuration of the five-legged transformer used in these tests did not allow us to reproduce this effect (an air gap is present between the three main limbs and the outer limbs).

These results show that neither the circuit breaker nor the winding coupling (wye or delta) seems to influence the residual flux as the different configurations produce very similar results. The interruption process can be different for larger transformer and high-voltage circuit breakers. A broader investigation of larger transformers is required before we are able to generalize these results.

#### B. Influence of shunt capacitor

The influence of the capacitance has been verified by attaching a variable shunt capacitor to the 15-kVA transformer. Fig. 9 shows the residual flux as function of the capacitance. The maximum residual flux is reduced by one third when a shunt capacitance of  $1 \mu\text{F}$  is attached to the transformer terminals. The line in Fig. 9 shows that the maximum residual flux decreases approximately proportional to the logarithm of the shunt capacitance:

$$\max(\lambda_0) \propto -\log(C) \quad (12)$$

Fig. 10 shows some measured flux-linked and current waveforms during ringdown transients. These waveforms qualitatively verify the behavior observed from the simulations: larger value of capacitance gives longer ringdown time and can drive

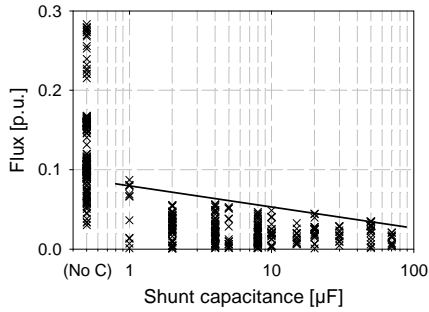


Fig. 9. Residual flux as function of the connected shunt capacitor (0-70  $\mu\text{F}$ ); measured on a 15-kVA three-legged transformer.

the core into high saturation. Residual fluxes (that could not be obtained with the simulation) are here present at the end of the transient. The hysteresis loop of one phase is also shown. During the ringdown transient current and flux-linked follow minor hysteresis loops. Higher number of loops are required for reaching steady state if a large capacitance is installed. The final point of the hysteresis loops lies on the zero current axis, but retain a certain value of flux.

#### IV. RESIDUAL FLUX-LINKED ESTIMATION AND INITIALIZATION

A hysteretic core model that can handle the demagnetization is required to accurately simulate the ringdown transient. Few hysteretic-nonlinear-inductor models appear to have the required property; two models that may be worth to verify with measurements are the Jiles-Atherton and Preisach models [11], [12]. However, their implementation in a simulation program is demanding both for modeling challenges and parameter estimation.

If the simulation interest is only inrush current estimation, the core model can be simpler because it does not need to represent the demagnetization transient. However, an accurate inrush estimation requires residual flux-linked initialization of every section of the core. The following recommendations should be taken into account:

- Maximum residual flux-linked for small distribution transformers lies in the range of 0.2-0.4 p.u. of the rated flux-linked, with slightly higher value for the central phase. If a shunt capacitance is connected to the transformer during the de-energization this range is decreased substantially.
- Residual fluxes in the different sections of the core of three-phase transformers are related on the basis of the core type. In three-legged transformers the residual fluxes of the three legs must sum to zero; the yokes share the same residual flux of the transformer leg that they are magnetically in parallel with. In five-legged transformers the residual fluxes of the three main legs plus the two outer legs must sum to zero. In banks of three single-phase transformers the residual flux can be initialized independently for each unit.

The extension of the results to medium/large power transformer is challenging due to the limited measurements presented in literature. Moreover, the use of improved core material in newer transformers reduces the validity of old

measurements. In a large Cigré survey (on more than 500 transformers) [13] carried out in 1984 the maximum residual flux is given only for two transformers (0.75 and 0.9 p.u.). Reference [2] dated 1986 suggests different remanent flux range cases varying between 0.4 and 0.8 p.u. The residual flux for a 545 MVA transformer is measured to be slightly higher than 0.4 p.u. (worst case out of 10 random de-energization) in [14]. One single measurement of the de-energization of a 170 MVA transformer is reported in [3] and has a residual flux of 0.31 p.u.

#### V. CONCLUSION

A ringdown transient can be easily replicated in the laboratory; however few if any of the existing EMTP type of models are capable of properly arriving at the value of the residual flux. A comparison between measured and simulated waveforms has not been presented due to the inferior quality of the ATP model used. The poor agreement between simulation and lab results shows the necessity of developing an improved model for ringdown transient simulation.

ATP simulations were useful to understand and qualitatively replicate the ringdown phenomena. A novel energy approach has been presented as a key to investigate the saturation behavior during ringdown; a transformer may be driven into heavy saturation by the energy stored in the capacitive elements of the circuit.

A proper residual flux estimation is difficult since the phase correlation between rated flux-linked and residual magnetization is no longer valid as the transformer size increases. Residual flux ranges and guidelines for flux initialization are given in the paper. When synchronized switching is used to mitigate inrush current, it is important to take into account that the central phase may have the highest peak of the residual flux. Thus, it is wise to avoid the energization of the central phase as first phase.

It has been observed that shunt capacitance has a main influence in residual magnetization and ringdown transient duration. If a large capacitance is connected to the transformer during the de-energization, longer time is required for reaching the end of the transient. This is an important aspect to take into account during protection scheme and relay reclosing-time strategies planning. A longer ringdown time also results in a lower residual flux.

#### APPENDIX

TABLE I  
GENERATOR STEP-UP TRANSFORMER TEST-REPORT.

Main data	[kV]	[MVA]	[A]	Coupling
HS	432	290	388	YN
LS	16	290	10465	d5
Open-circuit	$E_0$ [kV,(%)]	[MVA]	$I_0$ [%]	$P_0$ [kW]
LS	12(75)	290	0.05	83.1
	14(87.5)	290	0.11	118.8
	15(93.75)	290	0.17	143.6
	16(100)	290	0.31	178.6
	17(106.25)	290	0.67	226.5
Short-circuit	[kV]	[MVA]	$ek, er$ [%]	$P_k$ [kW]
HS/LS	432/16	290	14.6, 0.24	704.4

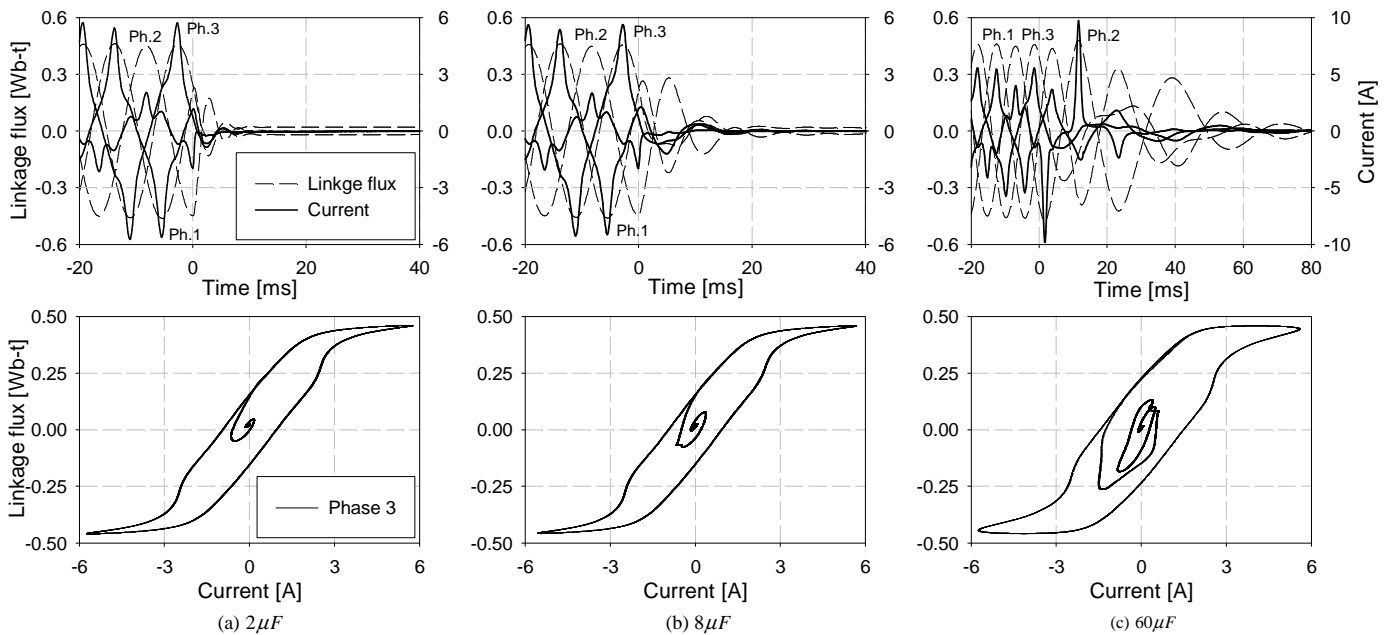


Fig. 10. Ringdown transient measured on a 15-kVA transformer; flux-linked, current waveforms and hysteresis loops.

#### REFERENCES

- [1] J. Holcomb, "Distribution transformer magnetizing inrush current," *Transactions of the American Institute of Electrical Engineers, Part III (Power Apparatus and Systems)*, vol. 80, no. 57, pp. 697–702, Dec. 1961.
- [2] R. Yacamini and A. Abu-Nasser, "The calculation of inrush current in three-phase transformers," *IEE Proceedings B (Electric Power Applications)*, vol. 133, no. 1, pp. 31–40, Jan. 1986.
- [3] Y. Husianycia and M. Rioual, "Determination of the residual fluxes when de-energizing a power transformer/comparison with on-site tests," *2005 IEEE Power Engineering Society General Meeting (IEEE Cat. No. 05CH37686)*, vol. 3, pp. 2492–2497, 2005.
- [4] R. Apolonio, J. C. de Oliveira, H. S. Bronzeado, and A. B. de Vasconcellos, "Transformer controlled switching: a strategy proposal and laboratory validation," in *11th International Conference on Harmonics and Quality of Power*, IEEE, Ed., Sep. 2004, pp. 625–630.
- [5] L. Prikler, G. Banfai, G. Ban, and P. Becker, "Reducing the magnetizing inrush current by means of controlled energization and de-energization of large power transformers," *Electric Power Systems Research EP-SRDN*, vol. 76, no. 8, pp. 642–649, May 2006.
- [6] L. M. Ganatra, P. G. Mysore, K. K. Mustaphi, A. Mulawarman, B. A. Mork, and G. Gopakumar, "Application of reclosing schemes in the presence of capacitor bank ringdown," *Proc Am Power Conf*, vol. 61-2, pp. 967–972, 1999.
- [7] F. de Leon and A. Semlyen, "A simple representation of dynamic hysteresis losses in power transformers," *IEEE Trans Power Delivery*, vol. 10, no. 1, pp. 315–321, 1995.
- [8] H. W. Dommel and et.al., *Electromagnetic Transients Program Reference Manual (EMTP Theory Book)*. Portland, OR: Prepared for BPA, Aug. 1986.
- [9] S. Denetière, J. Mahseredjian, M. Martinez, M. Rioual, A. Xémard, and P. Bastard, "On the implementation of a hysteretic reactor model in emtp," in *International Conference on Power Systems Transients, IPST03*, Ed., New Orleans, USA, 2003.
- [10] J. G. Frame, N. Mohan, and T. Liu, "Hysteresis modeling in an electro-magnetizing transient program," *IEEE Trans Power Appar Syst*, vol. PAS-101, pp. 3403–3412, Sep. 1982.
- [11] F. Liorzou, B. Phelps, and D. L. Atherton, "Macroscopic models of magnetization," *IEEE Trans. on Magnetics*, vol. 36, no. 2, pp. 418–428, Mar. 2000.
- [12] M. Popov, L. Van Der Sluis, G. C. Paap, and P. H. Schavemaker, "On a hysteresis model for transient analysis," *IEEE Power Engineering Review*, vol. 20, no. 5, pp. 53–55, May 2000.
- [13] E. Colombo and G. Santagostino, "Results of the enquiries on actual network conditions when switching magnetizing and small inductive currents and on transformer and shunt reactor saturation characteristics," *Electra*, vol. 94, pp. 35–53, May 1984.
- [14] H. Kohyama, K. Kamei, and H. Ito, "Application of controlled switching system for transformer energization taking into account a residual flux in transformer core," in *CIGRE SC A3&B3 Joint Colloquium in Tokyo*, 2005.

**Nicola Chiesa** was born in Cenate Sotto, Italy, on October 27, 1980. He received the M.S. degree in Electrical Engineering from Politecnico di Milano in 2005. In September 2005 he joined the Department of Electric Power Engineering at the Norwegian University of Science and Technology as a Ph.D. candidate.

**Alejandro Avendaño** was born in Tjuana, Mexico, on January 19, 1982. He received the B.S. degree in Electromechanical Engineering from Instituto Tecnológico de Tjuana in 2004. In 2005 he joined the Department of Electric & Computer Engineering at the Michigan Technological University as a Ph.D. candidate sponsored by the National Research Council of Mexico (CONACYT).

**Hans K. Høidalen** was born in Norway in 1967. He received his MSc and PhD from the Norwegian University of Science and Technology in 1990 and 1998 respectively. He is now a professor at the same institution with a special interest of electrical stress calculations and modeling.

**Bruce A. Mork** (M'82) was born in Bismarck, ND, on June 4, 1957. He received the BSME, MSEE, and Ph.D. from North Dakota State University in 1979, 1981 and 1992 respectively. He joined the faculty of Michigan Technological University in 1992, where he is now Associate Professor of Electrical Engineering, and Director of the Power & Energy Research Center.

**Dmitry Ishchenko** (M'04) was born in Krasnodar, Russia. He received his M.S. and Ph.D. degrees in Electrical Engineering from Kuban State Technological University, Russia in 1997 and 2002 respectively. In Feb. 2003 he joined the Electrical and Computer Engineering Department of MTU as a postdoctoral researcher.

**Andrew P. Kunze** (M'06) was born in Mahtowa, USA on November 28, 1983. He received a B.S. in Electrical Engineering from Michigan Technological University in 2006. He is currently pursuing an M.S. in Electrical Engineering at MTU.